Advances in Aircraft and Spacecraft Science, *Vol. 12, No. 2 (2025) 141-159*
https://doi.org/10.12989/aas.2025.12.2.141

Analysis of buckling behavior in advanced sandwich composite beams using a novel hyperbolic shear deformation theory

Mohammed Sid Ahmed Houari*[1], Ahmed Bakoura[2], Ali Belhocine[1], Abderahman Younsi[3], Ahmed Amine Daikh[1,4], Mohamed-Ouejdi Belarbi[5] and Abdelkrim Aid[6]

[1]Laboratoired'Etude des Structures et de Mécanique des Matériaux, Département de Génie Civil, Faculté des Sciences et de la Technologie, Université Mustapha Stambouli, B.P. 305, R.P. 29000 Mascara, Algérie
[2]Département de Génie Civil, Faculté d'Architecture et de Génie Civil, Université des Sciences et de la Technologie d'Oran, BP 1505 El M'naouer, USTO, Oran, Algeria
[3]Medea University, Medea, 26000, Algeria
[4]Artificial Intelligence Laboratory for Mechanical and Civil Structures, and Soil, University Centre of Naama, P.O. Box 66, Naama 45000, Algeria
[5]Laboratoire de Recherche en Génie Civil, LRGC, Université de Biskra, B.P. 145, R.P. 07000, Biskra, Algeria
[6]Department of Mechanical Engineering, Faculty of Science and Technology, University Mustapha Stambouli of Mascara, Mascara, Algeria

(Received December 31, 2024, Revised April 29, 2025, Accepted May 13, 2025)

Abstract. The buckling behavior of advanced sandwich composite beams is critical to their performance and stability, and understanding this behavior is essential for optimizing their design. This research aims to develop a new theory to investigate the buckling behavior of isotropic and functionally graded (FG) sandwich beams under various boundary conditions. The proposed theory eliminates the necessity of employing shear correction factors as it considers the parabolic variation of the shear stress distribution along the thickness. Based on Galerkin's method, a novel analytical solution is applied to solve the governing equilibrium equations. Considering that the material properties of functionally graded sandwich beams are graded in thickness according to a power-law distribution. A key aspect of this approach is to compare results obtained from the proposed theory with those derived from established higher-order shear deformation beam theories, intending to validate the accuracy and reliability of the new theory by comparing it with existing literature. In addition, the effects of different boundary conditions, FG material distribution, face-to-core thickness ratio, length-to-thickness ratio and volume fraction index on the critical buckling of FG sandwich beams are studied and discussed in detail. Our study showed that the shear deformation effect is remarkably significant for the case of thick or moderately thick beams. However, it is negligible in the case of slender beams. Finally, the presented findings and benchmark results offer a foundation for future research and design considerations within the domain of composite materials and structural engineering.

Keywords: advanced sandwich; beams; elastic buckling; functionally graded; shear deformation beam theory

*Corresponding author, Professor, E-mail: houarimsa@yahoo.fr

http://www.techno-press.org/?journal=aas&subpage=7 ISSN: 2287-528X (Print), 2287-5271 (Online)

1. Introduction

Sandwich construction is one of the most valuable composite constructions in the composites sector. Due to its lightweight structural approach and excellent stiffness and strength-to-weight ratios, it is frequently used in the aerospace and commercial industries (Vel *et al.* 2005). High specific resistance and bending stiffness-to-weight ratios set composite sandwich designs apart (Belouetar *et al.* 2009, Houari *et al.* 2008). The construction industry is likewise paying close attention to this composite material. It has recently been applied to civil engineering projects, including petrochemical structures, industrial buildings, automobile bridges, solar power plants, and nuclear reactor structures (Kolahchi *et al.* 2017, Bennoun *et al.* 2016). An interior layer that is somewhat thick and lightweight in the core material combines two comparatively thin and sturdy outside layers to create a structural sandwich (Sahu 2022). The sandwich construction has become even more appealing using composite materials for the face sheets, such as advanced functionally graded ceramic-metal composites (Wang and Shen 2012). One of the significant advantages of functionally graded materials (FGMs) over conventional materials is the elimination of the interface issues related to typical composite materials (Li *et al.* 2008). The smoothing of the stress distribution is another of these benefits. Consequently, several analyses of the statics, vibration and buckling of functionally graded structures (Shahmohammadi *et al.* 2020, Si *et al.* 2020, Liang *et al.* 2020, Karakoti *et al.* 2021, Taskin and Demirhan 2021, Sahoo *et al.* 2021, Foroutan and Dai 2022) have been conducted due to the rising significance of the structural components of functionally graded materials in the design of engineering structures. The expanding usage of these structures in industrial and other applications necessitated the development of new theories (Belabed *et al.* 2014, Belarbi *et al.* 2025, Fortas *et al.* 2022, Daikh *et al.* 2021, Daikh *et al.* 2021a, b, Elmascri *et al.* 2020, Emadi *et al.* 2021, She *et al.* 2020, Chinnapandi *et al.* 2022) to investigate the static, vibration, and buckling responses of FGM structures. A functionally graded beam is a fundamental component of numerous engineering structures and is utilized in numerous disciplines, including civil, mechanical, and space engineering. Diverse theories have been proposed to predict the mechanical behavior of FGM beams better. These beam theories can be categorized into three groups: the classical beam theory of Euler and Bernoulli (CBT), the first-order shear deformation theory (FSDT), and the higher-order shear deformation theories (HSDTs). The traditional beam theory does not account for the transverse shear strain, which is only studied in the context of thin beams. However, it is insufficient for moderately short and short beams, which require both transverse and normal strain consideration. The first-order shear deformation theory accounts for transverse shear deformation and produces correct findings for short and thin beams. Nevertheless, it requires a difficult-to-determine shear correction factor based on the geometry, material properties, and boundary conditions of each problem. HSDTs have been developed, do not require a shear correction factor, and provide more accurate forecasts than CBT and FSDT. These theories include higher-order terms for calculating in-plane displacement fields and satisfying the criterion of zero shear stress at the top and bottom surfaces of beams. As a result, this theory has been extensively applied to anticipate the behavior of beams manufactured from sophisticated composite materials. Numerous recent analytical and numerical investigations have been presented to precisely predict the mechanical behavior of functionally graded classical and sandwich beams, yielding essential physical and mechanical features of this structural type. Garg *et al.* (2021) and Sayyad and Ghugal (2019) conducted exhaustive analyses of functionally graded sandwich architectures. Literature (Thai et Kim 2015, Liew *et al.* 2019, Ghatage *et al.* 2020) provides another comprehensive evaluation of the current advancements of functionally

graded structures and their features and applications. Zenkour *et al.* (2010) propose an analysis of the bending response of a supported functionally graded (FG) viscoelastic sandwich beam with an elastic core sitting on Pasternak's elastic foundations. Nguyen and Nguyen (2015) used HSDT to develop a new way to analyze the free vibration, buckling, and statics of FG sandwich beams. The structural analysis of functionally graded (FG) sandwich beams has garnered significant attention due to their widespread use in aerospace, automotive, and civil engineering applications, where balancing accuracy and computational efficiency is paramount. Recent advancements in beam modeling have explored diverse approaches to address this challenge. Quasi-3D theories, which account for thickness-stretching effects critical for sandwich structures, have been employed to study bending, vibration, and buckling behaviors of FG beams (Karamanli 2017, Zenkour 2019), yet they often rely on complex constitutive equations. Layerwise models offer high precision for laminated composites by discretizing beams into sublayers (Carrera *et al.* 2011), but their computational cost limits scalability. Alternative methods, such as asymptotic variational techniques (Le *et al.* 2025) and numerical approaches like isogeometric B-splines (Shahmohammadi *et al.* 2020) or smoothed finite elements (Foroutan and Dai 2022), provide geometric flexibility but remain mesh-dependent. Innovations like Monte Carlo simulations combined with layer-wise Carrera Unified Formulation (CUF) models have also emerged to investigate mesoscale defects in variable-angle tow laminates (Pagani nd Sánchez-Majano 2022). Despite these developments, analytical solutions for FG sandwich beams under varied boundary conditions remain scarce, particularly those that avoid simplifying assumptions or excessive discretization. This gap underscores the need for robust models that integrate thickness-stretching effects and diverse boundary conditions, as demonstrated by Karamanli's (2017) use of quasi-3D shear deformation theory with symmetric smoothed particle hydrodynamics to analyze two-directional FG sandwich beams.

To the best of the authors' knowledge, no existing publication addresses the buckling response of functionally graded (FG) sandwich beams under various boundary conditions using an analytical solution based on the new shear deformation theory. In this context, the primary objective and the key novelty of this study are to develop an efficient analytical model, based on the Galerkin method, for investigating the buckling behavior of FG sandwich beams with different boundary conditions. Novel buckling load solutions are derived using a newly proposed two-variable hyperbolic shear deformation beam theory. The effects of several influential parameters, including boundary conditions, FG material distribution, face-to-core thickness ratio, length-to-thickness ratio, and volume fraction index, are thoroughly examined. Benchmark results are provided for the first time, offering valuable references for future research in this area.

2. Theoretical formulation

The properties of FGM vary continuously due to gradually changing the volume fraction of the constituent materials, usually in the thickness direction only. A power-law function is commonly used to describe these variations in material properties. The isotropic FG beams and FG sandwich beams made of power-law FGMs are discussed.

2.1 FG sandwich beams

Consider a beam shown in Fig. 1 with length $L$and uniform section . The beam is

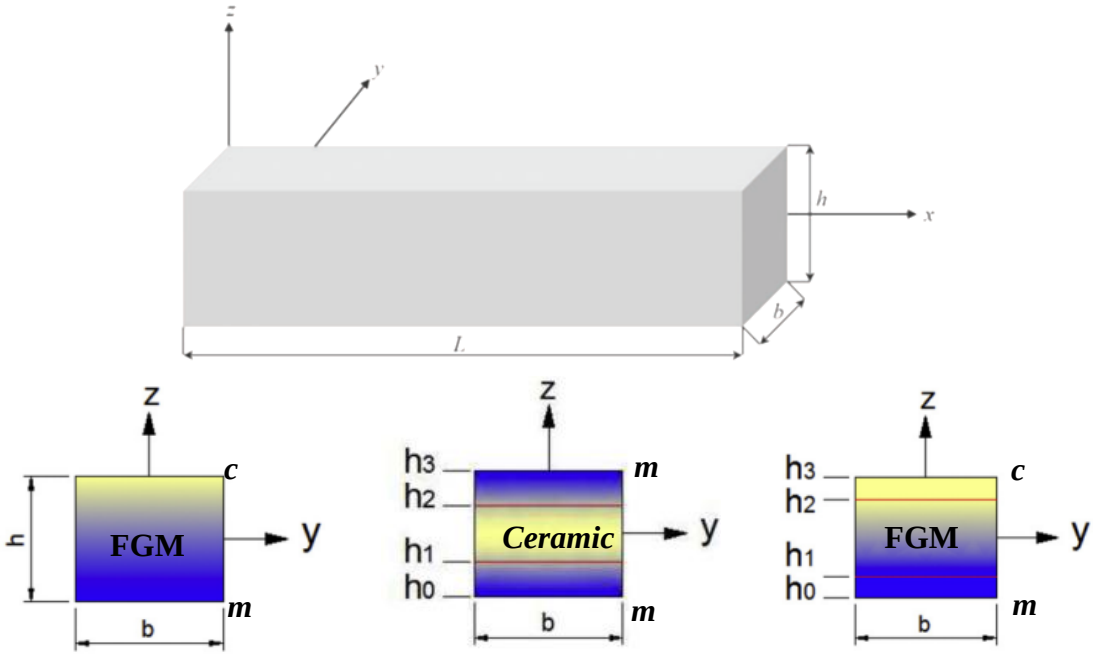

Fig. 1 Geometry of isotropic and FG sandwich beams

constructed of ceramic and metal isotropic materials whose characteristics fluctuate gradually with depth according to their volume percentages. Three types of FG beams are considered: isotropic (type A), sandwich beams with FG faces and homogeneous core (type B), and sandwich beams with FG core and homogeneous faces (type C).

2.1.1 Type A: İsotropic FG beams

The beam of type A is graded from metal located at the bottom surface to ceramic material at the top surface (Fig. 1(b)). The volume fraction of ceramic material V_c is given as follows

$$V_c(z) = \left(\frac{2z+h}{2h}\right)^k \tag{1}$$

where k is the scalar parameter, which is positive and $z \in [-h/2, h/2]$.

2.1.2 Type B: Sandwich beams with FG faces and homogeneous core

This type has faces that vary from metal to ceramic, and the core is made of an isotropic ceramic (Fig. 1(c)). The volume fraction of the FGMs is assumed to obey a power-law function along the thickness direction

$$V^{(1)} = \left(\frac{z-h_1}{h_2-h_1}\right)^k, z \in [h_1, h_2] \tag{2a}$$

$$V^{(2)} = 1, z \in [h_2, h_3] \tag{2b}$$

$$V^{(3)} = \left(\frac{z - h_4}{h_3 - h_4}\right)^k, z \in [h_3, h_4] \tag{2c}$$

where $V^{(n)}$, $(n = 1,2,3)$ denotes the volume fraction function of layer n; k is the volume fraction index ($0 \leq k \leq +\infty$), which dictates the material variation profile through the thickness.

2.1.3 Type C: Sandwich beams with FG core and homogeneous faces

The volume fraction of the FGMs is assumed to obey a power-law function along the thickness direction

$$V^{(1)} = 0, z \in [h_1, h_2] \tag{3a}$$

$$V^{(2)} = \left(\frac{z - h_2}{h_3 - h_2}\right)^k, z \in [h_2, h_3] \tag{3b}$$

$$V^{(3)} = 1, z \in [h_3, h_4] \tag{3c}$$

The effective material properties, like Young's modulus E and Poisson's ratio v can be expressed by the rule of mixture as

$$P^{(n)}(z) = P_2 + (P_1 - P_2)V^{(n)} \tag{4}$$

where $P^{(n)}$ is the effective material property of FGM of layer n. For type B, P_1 and P_2 are the properties of the top and bottom faces of layer 1, respectively, and vice versa for layer 3 depending on the volume fraction $V^{(n)}$, $(n = 1,2,3)$. For type C, P_1 and P_2 are the properties of layer 3 and layer 1, respectively. For simplicity, the Poisson's ratio of the beam is assumed to be constant in this study, as its effect on deformation is significantly smaller than that of Young's modulus (Daikh *et al.* 2021, Daikh *et al.* 2022, Hirane *et al.* 2021).

2.2 Basic assumptions

The assumptions of the proposed theory are as follows:

(i) The displacements are small in comparison with the beam thickness and, therefore, strains involved are infinitesimal;

(ii) The transverse displacement $\boldsymbol{w}$ includes two components bending w_b and shear w_s. The two components are functions of coordinate $\boldsymbol{x}$ only

$$w(x) = w_b(x) + w_s(x) \tag{5}$$

The displacements u in the x-direction consist of extension, bending, and shear components.

$$u = u_0 + u_b + u_s \tag{6}$$

The bending component u_b is assumed to be similar to the displacement given by the classical beam theory. Therefore, the expression for u_b can be given as

$$u_b = -z\frac{\partial w_b}{\partial x} \tag{7}$$

The shear component u_s gives rise, in conjunction with w_s, to the sinusoidal variations of shear strain γ_{xz} and hence to shear stress τ_{xz} through the thickness of the beam in such a way that shear

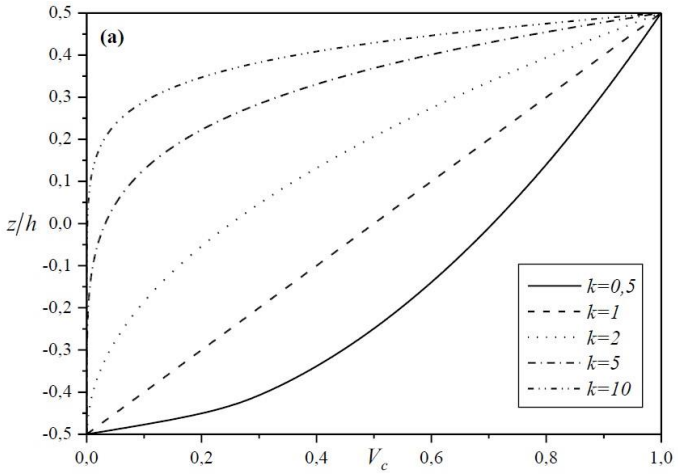

(a) Type A

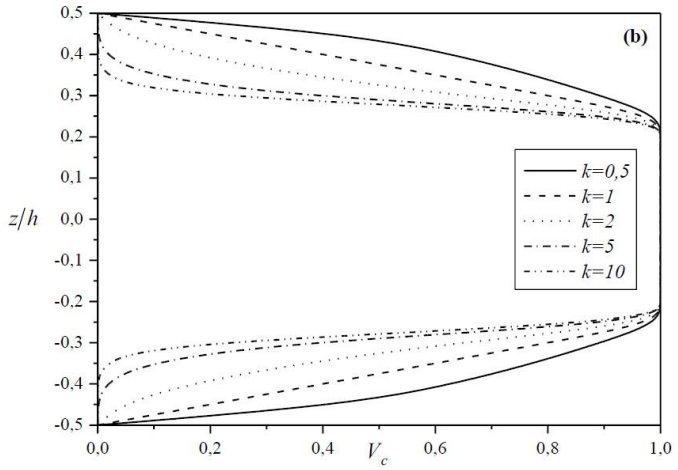

(b) Type B

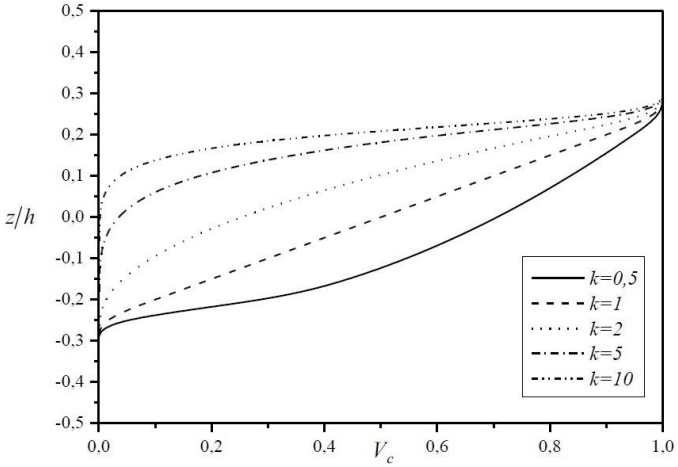

(c) Type C

Fig. 2 Distribution of ceramic material through the beam depth according to the power-law form

stress τ_{xz} is zero at the top and bottom faces of the beam. Consequently, the expression for u_s can be given as

$$u_s = -f(z)\frac{\partial w_s}{\partial x} \tag{8}$$

where

$$f(z) = \frac{\frac{h}{\pi}sinh\left(\frac{h}{\pi}z\right)-z}{\left[cosh\left(\frac{\pi}{2}\right)-1\right]} \tag{9}$$

2.3 Kinematics and constitutive equations

Based on the assumptions made in the preceding section, the displacement field can be obtained using Eqs. (5)-(9) as

$$\begin{gathered} u(x,z) = u_0(x) - z\frac{\partial w_b}{\partial x} - f(z)\frac{\partial w_s}{\partial x} \\ w(x,z) = w_b(x) + w_s(x) \end{gathered} \tag{10}$$

The strains associated with the displacements in Eq. (10) are

$$\begin{gathered} \varepsilon_x = \varepsilon_x^0 + zk_x^b + f(z)k_x^s \\ \gamma_{xz} = g(z)\gamma_{xz}^0 \\ g(z) = 1 - f'(z) \end{gathered} \tag{11}$$

where

$$\varepsilon_x^0 = \frac{\partial u_0}{\partial x}, k_x^b = \frac{\partial^2 w_b}{\partial x^2}, k_x^s = \frac{\partial^2 w_s}{\partial x^2}, \gamma_{xz}^0 = \frac{\partial w_s}{\partial x} \tag{12}$$

By assuming that the material of FG beam obeys Hooke's law, the stresses in the beam become

$$\sigma_x = Q_{11}(z)\varepsilon_x \text{and} \tau_x = Q_{55}(z)\gamma_{xz} \tag{13}$$

where

$$Q_{11}(z) = \frac{E(z)}{(1-\nu^2)} \text{ and } Q_{55}(z) = \frac{E(z)}{2(1+\nu)} \tag{14}$$

2.4 Equations of motion

The equilibrium equations can be determined by applying the principle of total potential energy as follows

$$\delta(\Pi_1 + \Pi_2) = 0 \tag{15}$$

Here $\delta\Pi_1$ denotes strain energy and $\delta\Pi_2$ work done by external forces.
The Eq. (13) given as

$$\begin{aligned} \delta\Pi_1 + \delta\Pi_2 = \delta U &= \int_0^L \int_{-\frac{h}{2}}^{\frac{h}{2}} (\sigma_x \delta\,\varepsilon_x + \tau_{xz}\delta\,\gamma_{xz})\; dxdz + \int_0^L \overline{N}\frac{d(w_b+w_s)}{dx}\frac{d\delta(w_b+w_s)}{dx}dx \\ &= \int_0^L \left(N\frac{d\delta u_0}{dx} - M_b\frac{d^2\delta w_b}{dx^2} - M_s\frac{d^2\delta w_s}{dx^2} + Q\frac{d\delta w_s}{dx}\right) dx \\ &\quad + \int_0^L \overline{N}\frac{d(w_b+w_s)}{dx}\frac{d\delta(w_b+w_s)}{dx}dx = 0 \end{aligned} \tag{16}$$

where N, M_b,M_s and Q are the stress resultants defined as

$$(N, M_b, M_s) = \int_{-h/2}^{h/2} \big(1, z, f(z)\big)\sigma_x dz, \quad \text{and} \quad Q = \int_{-h/2}^{h/2} \tau_{xz} g(z) dz \tag{17}$$

The equations of equilibrium are obtained by employing the integration by parts for Eq. (16) and then setting the coefficients of δu_0, δw_b and δw_s to zero, separately. Then, the equilibrium equations of the current theory are obtained as

$$\begin{aligned} &\delta u_0: \ \frac{dN}{dx} = 0 \\ &\delta w_b: \ \frac{d^2 M_b}{\partial x^2} + \overline{N}\left(\frac{\partial^2 (w_b + w_s)}{\partial x^2}\right) = 0 \\ &\delta w_s: \ \frac{d^2 M_s}{\partial x^2} + \frac{dQ}{dx} + \overline{N}\left(\frac{\partial^2 (w_b + w_s)}{\partial x^2}\right) = 0 \end{aligned} \tag{18}$$

Eq. (18) can be expressed in terms of displacements (u_0,w_b,w_s) by using Eqs. (11), (13), and (17) as follows

$$A_{11}\frac{d^2 u_0}{dx^2} - B_{11}\frac{d^3 w_b}{dx^3} - B_{11}^s \frac{d^3 w_s}{dx^3} = 0, \tag{19a}$$

$$B_{11}\frac{d^3 u_0}{dx^3} - D_{11}\frac{d^4 w_b}{dx^4} - D_{11}^s \frac{d^4 w_s}{dx^4} + \overline{N}\left(\frac{d^2 (w_b + w_s)}{dx^2}\right) = 0, \tag{19b}$$

$$B_{11}^s\frac{d^3 u_0}{dx^3} - D_{11}^s\frac{d^4 w_b}{dx^4} - H_{11}^s \frac{d^4 w_s}{dx^4} + A_{55}^s \frac{d^2 w_s}{dx^2} + \overline{N}\left(\frac{d^2 (w_b + w_s)}{dx^2}\right) = 0, \tag{19c}$$

where A_{11}, B_{11}, etc., are the beam stiffness, defined by

$$\big(A_{11}, B_{11}, D_{11}, B_{11}^b, D_{11}^b, H_{11}^b\big) = \int_{-h/2}^{h/2} Q_{11}(1, z, z^2, f(z), z\, f(z), f^2(z))\, dz \quad \text{and} \tag{20a}$$

$$A_{55}^s = \int_{-h/2}^{h/2} Q_{55}[g(z)]^2 dz, \tag{20b}$$

3. Analytical solution

The exact solution of Eq. (19) for the FG beam under various boundary conditions can be constructed. The boundary conditions for an arbitrary edge with simply supported and clamped edge conditions are:

- Clamped (C)

$$u_0 = w_b = \frac{\partial w_b}{\partial x =} w_s = \frac{\partial w_s}{\partial x = 0 at x = 0, L} \tag{21a}$$

- Simply supported (S)

$$w_b = w_s = 0 at x = 0, L \tag{21b}$$

The following representation for the displacement quantities, that satisfy the above boundary

conditions, is appropriate in the case of our problem

$$\begin{Bmatrix} u_0 \\ w_b \\ w_s \end{Bmatrix} = \begin{Bmatrix} U_m X_m^{'} \\ W_{bm} X_m \\ W_{sm} X_m \end{Bmatrix} \tag{22}$$

where U_m, W_{bm} and W_{sm} are arbitrary parameters to be determined. The function $X_m(x)$ is suggested by [31] to satisfy at least the geometric boundary conditions given in Eqs. (21) and represents the approximate shapes of the deflected beam. These functions, for the different cases of boundary conditions, are given as:

- For Simply supported beam (SS)

$$X_m(x) = sin(\lambda x) \text{ and } \lambda = \frac{m\pi}{L} \tag{23}$$

- For Clamped-clamped beam (CC)

$$X_m(x) = 1 - cos(\lambda x) \text{ and } \lambda = \frac{2m\pi}{L} \tag{24}$$

- For Clamped-free beam (CC)

$$X_m(x) = 1 - cos(\lambda x) \text{ and } \lambda = \frac{2m\pi}{L} \tag{25}$$

Substituting Eqs. (22), (23), (24), and (25) into Eq. (19), the analytical solutions can be obtained; for buckling problems and the buckling equation can be expressed as

$$([K] - [N])\{\Delta\} = \{0\} \tag{26}$$

Where

$$[K] = \begin{bmatrix} a_{11} & a_{12} & a_{13} \\ a_{21} & a_{22} & a_{23} \\ a_{31} & a_{32} & a_{33} \end{bmatrix} \tag{27}$$

And

$$[N] = \begin{bmatrix} 0 & 0 & 0 \\ 0 & \overline{N}\alpha_3 & \overline{N}\alpha_3 \\ 0 & \overline{N}\alpha_3 & \overline{N}\alpha_3 \end{bmatrix}, \{\Delta\} = \begin{Bmatrix} U_m \\ W_{bm} \\ W_{sm} \end{Bmatrix}, \tag{28}$$

Where

$$\begin{gathered} a_{11} = A_{11}\alpha_4, a_{12} = -B_{11}\alpha_4, a_{13} = -B_{11}^s\alpha_4, a_{21} = B_{11}\alpha_5, a_{22} = -D_{11}\alpha_5, \; a_{23} = \\ -D_{11}^s\alpha_5, a_{31} = B_{11}^s\alpha_5, \;\; a_{23} = -D_{11}^s\alpha_5 \;\; , a_{33} = -H_{11}^s\alpha_5 + A_{55}^s\alpha_3, \\ \text{with } (\alpha_1, \alpha_3, \alpha_5) = \int_0^L \left(X_m, X_m^{''}, X_m^{''''}\right) X_m dx \\ (\alpha_2, \alpha_4) = \int_0^L \left(X_m^{'}, X_m^{'''}\right) X_m^{'} dx \end{gathered} \tag{29}$$

4. Numerical results and discussion

In this section, the study's accuracy is validated through numerical examples, and the critical buckling loads of isotropic and FG sandwich beams are determined. Three types of FG beams (A,

Table 1 Comparison of the nondimensional critical buckling load ($\bar{N}_{cr}$) of FG beams with various boundary conditions ($L/h = 5$ and 10 type A)

L/h	BC	Theory	k					
			0	0.5	1	2	5	10
5	S-S	Present	48.6436	31.8942	24.6044	19.0783	15.6209	14.0531
		HypSDT*	48.8406	32.0013	24.6894	19.1577	15.7355	14.1448
		TSDT **	48.8401	32.0094	24.6911	19.1605	15.7400	14.1468
		FSDT ***	48.8350	31.9670	24.6870	19.2450	16.0240	14.4270
	C-C	Present	152.7172	102.6169	79.7461	60.9974	46.7383	41.0522
		HypSDT *	154.5610	103.7167	80.5940	61.7666	47.7174	41.7885
		TSDT **	154.5500	103.7490	80.6087	61.7925	47.7762	41.8042
		FSDT ***	154.3500	103.2200	80.4980	62.6140	50.3840	44.2670
10	S-S	Present	52.2508	33.9748	26.1464	20.3680	17.0745	15.4995
		HypSDT *	52.3083	34.0002	26.1707	20.3909	17.1091	15.5278
		TSDT **	52.3082	34.0087	26.1727	20.3936	17.1118	15.5291
		FSDT ***	52.3090	33.9960	26.1710	20.4160	17.1920	15.6120
	C-C	Present	194.5742	127.5768	98.41748	76.3132	62.4836	56.2123
		HypSDT *	195.3623	128.0053	98.7885	76.6538	62.9580	56.5926
		TSDT **	195.3610	128.0500	98.7868	76.6677	62.9786	56.5971
		FSDT ***	195.3400	127.8700	98.7490	76.9800	64.0960	57.7080

* Nguyen *et al.* (2015) ** Vo *et al.* (2014) *** Nguyen *et al.* (2013)

B, and C) are created by combining isotropic ceramic Al_2O_3 and metal Al. The material properties of Al_2O_3 are: $E_c = 380$ GPa, $v_c = 0.3$, $\rho_c = 3960$ kg/m^3, and those of Al are: $E_c = 70$ GPa, $v_m = 0.3$, $\rho_m = 2702$ kg/m^3. The effects of the power-law index, span-to-depth ratio, skin-core-skin thickness ratios, and boundary conditions on the buckling behavior of the isotropic and FG sandwich beams are discussed in detail. Two boundary conditions (BC) are considered: C-C and S-S. To simplify the analysis, the non-dimensional critical buckling loads are defined as

$$\bar{N}_{cr} = \frac{12 N_{cr} L^2}{E_m h^3} \tag{30}$$

As the first example, Table 1 provides the comparison of the critical buckling loads of FG beams (type A) under two boundary conditions. These values are computed across different power-law index and compared to the solutions obtained from the higher-order shear deformation beam theories (Vo *et al.* 2014, Nguyen *et al.* 2015, Nguyen *et al.* 2013). The proposed theory's solutions for deep and slender beams are in perfect agreement with those derived from earlier results.

Fig. 3 illustrates the variation of the critical buckling load with respect to the power-law index and the span-to-depth ratio for FG beams under two boundary conditions. The curve representing the clamped-clamped boundary condition is consistently higher than the curve for simply-simply supported beams. It is observable that the results decrease with an increase in the power-law index. To further validate the proposed theory, a comparison is made between the critical buckling loads of type B sandwich beams obtained from this study and those reported by Vo *et al.* (2014), Nguyen *et al.* (2015) using the HSBT method. The comparison, presented in Tables 2 and 3,

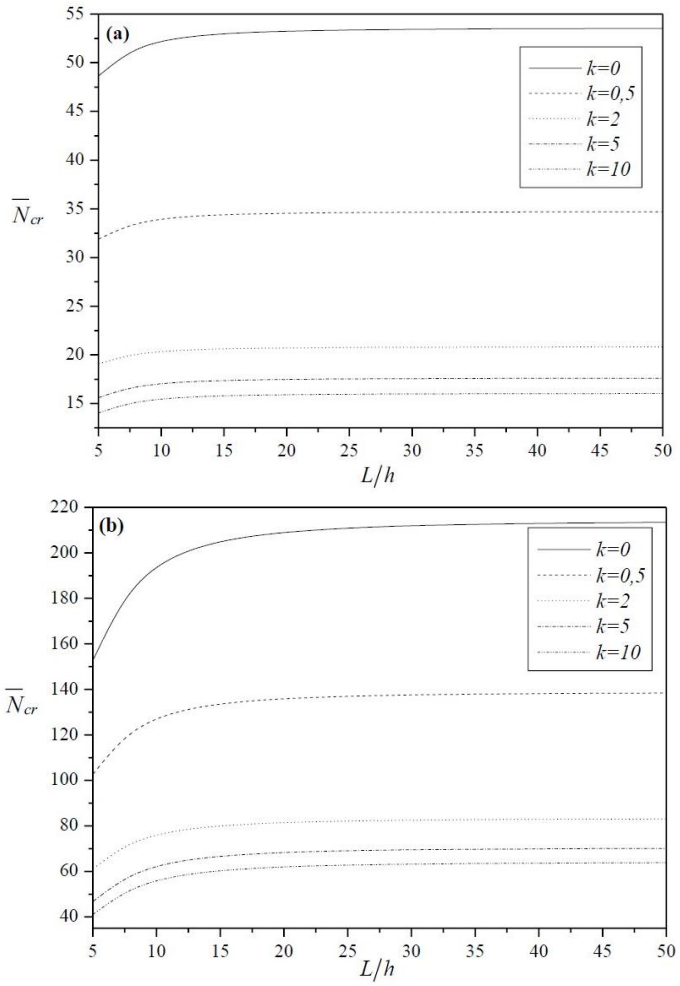

Fig. 3 Variation of the nondimensional critical buckling load of FG beams with respect to the span-to-depth ratio *L/h* (type A): (a) S-S; (b) C-C

considers six different values of the skin-core-skin thickness ratios and various power-law index values. The results demonstrate a remarkable agreement between the present theory and the HSBT approach for type B beams. This agreement serves as evidence that the proposed theory is suitable and effective for analyzing the buckling behavior of sandwich beams. Notably, the (1-0-1) and (1 2-1) sandwich beams exhibit the lowest and highest critical buckling loads, respectively. This trend can be attributed to the volume fractions of the ceramic phase, where the (1-0-1) beam has the lowest volume fraction and the (1-2-1) beam has the highest. Table 4 presents a comparison of the critical buckling loads for (1-2-1) and (2-2-1) sandwich beams of type C with results obtained from Nguyen *et al.* (2015) hyperbolic shear deformation beam theory. The analytical model proposed in this study demonstrates excellent agreement with the reference solution by Nguyen *et al.* (2015). Furthermore, our findings highlight the significant impact of shear deformation in thick or moderately thick beams, while its influence is negligible in thin beams. As a result of the increased ceramic portion, the (1-2-1) sandwich beam's results are greater than those of the (2-2-1)

Table 2 Nondimensional critical buckling load ($\bar{N}_{cr}$) of FG sandwich beams with various boundary conditions ($L/h = 5$, type B)

BC	k	Theory	1-0-1	2-1-2	2-1-1	1-1-1	2-2-1	1-2-1
S-S	0	Present	48.6436	48.6436	48.6436	48.6436	48.6436	48.6436
		TSBT **	48.5959	48.5959	48.5959	48.5959	48.5959	48.5959
		HypSDT *	48.5964	48.5964	48.5964	48.5964	48.5964	48.5964
	0.5	Present	27.8902	30.0599	31.0960	31.9011	33.2733	34.7766
		TSBT **	27.8574	30.0301	31.0728	31.8784	33.2536	34.7653
		HypSDT *	27.8380	30.0146	31.0577	31.8650	33.2336	34.7546
	1	Present	27.8902	22.2360	23.5424	24.5769	26.3748	28.4476
		TSBT **	19.6525	22.2108	23.5246	24.5596	26.3611	28.4447
		HypSDT *	19.6541	22.2121	23.5250	24.5602	26.3611	28.4440
	2	Present	13.6084	15.9394	17.3415	18.3753	20.3876	22.7873
		TSBT **	13.5801	15.9152	17.3249	18.3587	20.3750	22.7863
		HypSDT *	13.5820	15.9167	17.3254	18.3596	20.3751	22.7859
	5	Present	10.1813	11.6955	13.0456	13.7413	15.7465	18.0961
		TSBT **	10.1460	11.6676	13.0270	13.7212	15.7307	18.0914
		HypSDT *	10.1488	11.6697	13.0279	13.7226	15.7313	18.0915
	10	Present	9.4912	10.5664	11.8566	12.2835	14.2173	16.3863
		TSBT **	9.4515	10.5348	11.8370	12.2605	14.1995	16.3783
		HypSDT *	9.4543	10.5370	11.8380	12.2621	14.2002	16.3789
C-C	0	Present	152.7172	152.7172	152.7172	152.7172	152.7172	152.7172
		TSBT **	152.1470	152.1470	152.1470	152.1470	152.1470	152.1470
		HypSDT *	152.1588	152.1588	152.1588	152.1588	152.1588	152.1588
	0.5	Present	93.2808	100.3532	103.2066	105.9692	109.8611	114.3407
		TSBT **	92.8833	99.9860	102.9120	105.6790	109.6030	114.1710
		HypSDT *	92.8202	99.9361	102.8605	105.6331	109.5284	114.1312
	1	Present	67.8521	76.5805	80.3954	84.0426	89.4042	95.7923
		TSBT **	67.4983	76.2634	80.1670	83.8177	89.2208	95.7287
		HypSDT *	67.5184	76.2801	80.1730	83.8267	89.2223	95.7230
	2	Present	48.0610	56.5190	60.8208	64.6392	70.9246	78.5900
		TSBT **	47.7010	56.2057	60.6056	64.4229	70.7563	78.5608
		HypSDT *	47.7247	56.2259	60.6127	64.4352	70.7590	78.5570
	5	Present	35.9920	42.3717	46.6180	49.5433	56.0347	63.8519
		TSBT **	35.5493	42.0033	46.3743	49.2763	55.8271	63.7824
		HypSDT *	35.5811	42.0298	46.3852	49.2949	55.8338	63.7847
	10	Present	32.7772	38.4122	46.6180	44.6463	50.9672	58.3572
		TSBT **	32.3019	37.9944	42.1935	44.3374	50.7315	58.2461
		HypSDT *	32.3345	38.0239	42.2062	44.3593	50.7406	58.2532

* Nguyen *et al.* (2013) ** Vo *et al.* (2014)

one. Maximum values are observed for k=0, while minimum values are noted for k=10.

Furthermore, Figs. 4 and 5 illustrate the impact of the volume fraction index (k) and face-to-core thickness ratio on the non-dimensional critical buckling loads for both hardcore and FG core

Table 3 Nondimensional critical buckling load ($\bar{N}_{cr}$) of FG sandwich beams with various boundary conditions ($L/h = 20$, type B).

BC	k	Theory	1-0-1	2-1-2	2-1-1	1-1-1	2-2-1	1-2-1
S-S	0	Present	53.2397	53.2397	53.2397	53.2397	53.2397	53.2397
		TSBT **	53,2364	53,2364	53,2364	53,2364	53,2364	53,2364
		HypSDT *	53,2364	53,2364	53,2364	53,2364	53,2364	53,2364
	0.5	Present	29.7198	32.0556	33.2391	34.0878	35.6417	37.3166
		TSBT **	29,7175	32,2629	33,2376	34,0862	35,6405	37,3159
		HypSDT *	29,6965	32,0368	33,2217	34,0722	35,6202	37,3054
	1	Present	20.7232	23.4228	24.8805	25.9600	27.9546	30.2308
		TSBT **	20,7212	23,4211	24,8796	25,9588	27,9540	30,2307
		HypSDT *	20,7213	23,4212	24,8793	25,9588	27,9537	30,2306
	2	Present	14.1992	16.6066	18.1411	19.2010	21.3932	23.9900
		TSBT **	14,1973	16,6050	18,1404	19,3116	21,3927	23,9900
		HypSDT *	14,1974	16,6051	18,1400	19,2000	21,3923	23,9899
	5	Present	10.6195	12.0902	18.1411	19.2010	16.3839	18.8877
		TSBT **	10,6171	12,0883	13,5523	14,2284	16,3834	18,8874
		HypSDT *	10,6176	12,0886	13,5520	14,2285	16,3829	18,8874
	10	Present	9.9875	10.9096	12.3092	12.6834	14.7531	17.0448
		TSBT **	9,9847	10,9075	12,3084	12,6819	14,7525	17,0443
		HypSDT *	9,9850	10,9075	12,3081	12,6820	14,7520	17,0445
C-C	0	Present	209.0032	209.0032	209.0032	209.0032	209.0032	209.0032
		TSBT **	208,9510	208,9510	208,9510	208,9510	208,9510	208,9510
		HypSDT *	208,9515	208,9515	208,9515	208,9515	208,9515	208,9515
	0.5	Present	117.3381	126.5404	131.1467	134.5052	140.5636	147.1151
		TSBT **	117,3030	126,5080	131,1240	134,4810	140,5450	147,1040
		HypSDT *	117,2200	126,4422	131,0594	134,4255	140,4622	147,0614
	1	Present	82.0233	92.7010	98.4024	102.6832	110.4937	119.4248
		TSBT **	81,9927	92,6741	98,3880	102,6650	110,4830	119,4220
		HypSDT *	81,9944	92,6754	98,3839	102,6655	110,4792	119,4215
	2	Present	56.3075	65.8746	71.9007	76.1195	84.7362	94.9568
		TSBT **	56,2773	65,8489	71,8900	76,1020	84,7291	94,9563
		HypSDT *	56,2793	65,8505	71,8837	76,1030	84,7230	94,9558
	5	Present	42.1152	48.0363	53.7934	56.5168	65.0089	74.8950
		TSBT **	42,0775	48,0070	53,7820	56,4958	65,0007	74,8903
		HypSDT *	42,0814	48,0095	53,7751	56,4973	64,9930	74,8903
	10	Present	39.5360	43.3565	48.8636	50.4053	58.5706	67.6352
		TSBT **	39,4930	43,3233	48,8510	50,3811	58,5607	67,6270
		HypSDT *	39,4962	43,3252	48,8443	50,3827	58,5529	67,6281

* Nguyen *et al.* (2013) ** Vo *et al.* (2014)

sandwich beams. The figures show that, for simply supported beams and clamped-clamped beams with (*L/h*=10), the non-dimensional critical buckling load values decrease as the volume fraction index for FG sandwich beams with isotropic hardcore and FG core increases. This trend can be

Table 4 Nondimensional critical buckling load ($\bar{N}_{cr}$) of FG sandwich beams with various boundary conditions (type C)

Scheme	L/h	BC	Theory	k					
				0	0,5	1	2	5	10
1-2-1	5	S-S	Present	27.9682	23.0285	20.7987	18.9525	17.6586	17.2611
			HypSDT*	27,9314	22,9869	20,7762	18,9588	17,7320	17,3775
		C-C	Present	95.0673	77.9610	69.7715	62.1963	55.2794	52.3615
			HypSDT *	94,6117	77,5129	69,4877	62,2249	55,9446	53,3734
	20	S-S	Present	29.6145	24.4239	22.1401	20.3575	19.3580	19.1962
			HypSDT *	29,6120	24,4140	22,1386	20,3581	19,3639	19,2058
		C-C	Present	117.0780	96.5245	87.4310	80.2386	75.9668	75.0971
			HypSDT *	117,0384	96,4573	87,4069	80,2465	76,0539	75,2379
2-2-1	5	S-S	Present	21.5747	19.5184	18.5846	17.7650	17.0808	16.8151
			HypSDT *	21,5207	19,4909	18,5897	17,8178	17,1942	16,9422
		C-C	Present	74.7598	65.5907	60.8345	55.9279	50.9805	48.9455
			HypSDT *	74,0960	65,2766	60,8501	56,4008	51,9303	49,9605
	20	S-S	Present	22.6751	20.7627	19.9834	19.4251	19.1412	19.0739
			HypSDT *	22,6714	20,7578	19,9839	19,4292	19,1504	19,0848
		C-C	Present	89.7835	82.0038	78.7462	76.2722	74.7571	74.2949
			HypSDT *	89,7255	81,9647	78,7529	76,3344	74,8949	74,4533

* Nguyen *et al.* (2013)

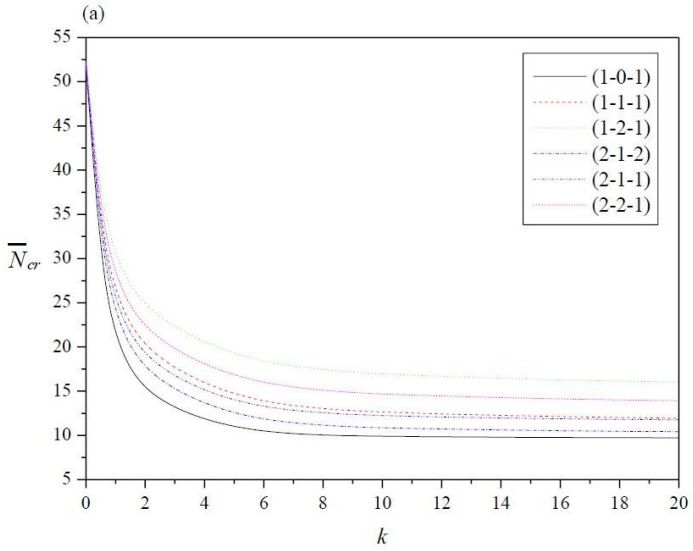

Fig. 4 Effect of the volume fraction index (k) on the nondimensional critical buckling load $\bar{N}_{cr}$ of FG sandwich beams type B: (a) simply supported beam and (b) clamped–clamped beam ($L/h = 10$)

attributed to the fact that higher values of the volume fraction index (k) correspond to a smaller ceramic component and a higher portion of the metal phase, resulting in reduced stiffness and softer FG sandwich beams. Additionally, the figures reveal that, for hardcore FG sandwich beams,

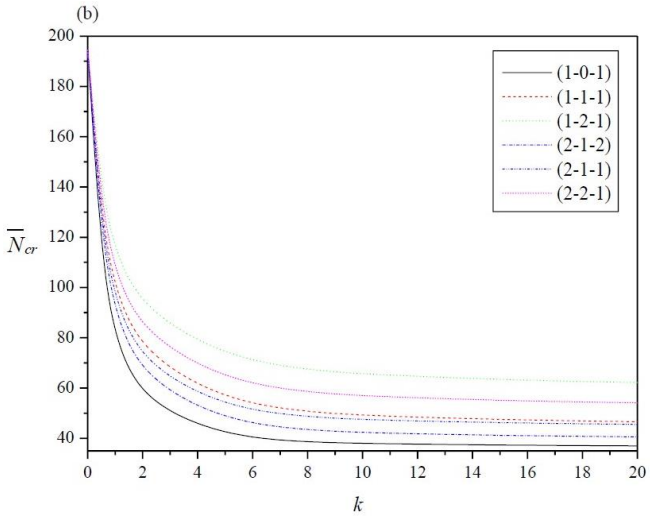

Fig. 4 Continued

the non-dimensional critical buckling loads are highest for the (1-2-1) beam and lowest for the (1-0-1) beam for type B. Similarly, for core FG sandwich beams, the critical buckling loads reach their maximum for the (1-2-1) beam and remain constant for the (1-0-1) beams. Unlike numerical methods, it provides robust analytical solutions for complex boundaries (e.g., clamped-free) without excessive discretization. These advances enable optimized lightweight designs in aerospace, civil, and energy sectors, bridging physical precision with industrial efficiency.

5. Conclusions

This research aimed to develop an efficient analytical model based on the Galerkin method to study the buckling behavior of FG sandwich beams with various boundary conditions. The proposed model provides novel solutions for buckling loads based on a new two-variable hyperbolic shear deformation beam theory. The research investigated several aspects of various boundary conditions, FG material distribution, face-to-core-thickness ratio, length-to-thickness ratio, and volume fraction index, and their impact on the analytical solutions.

The novel shear deformation theory presented in this research offers a significant improvement over existing research, providing a more accurate and efficient method for predicting the buckling behavior of FG sandwich beams. Finally, the findings of this research have significant implications for the design and optimization of FG sandwich beams, as they provide a reliable method for predicting their buckling behavior under mechanical loads, enabling engineers to create safer and more efficient structures. Finally, the formulation lends itself particularly well to the study of several problems related to the bending, vibration, and dynamic behavior of isotropic, classical, and advanced composite macro/nanostructures (Mouffoki *et al.* 2017, Sabherwal *et al.* 2024, Daikh *et al.* 2024, Merzouki *et al.* 2022, Mokhefi *et al.* 2024). Additionally, this approach supports the analysis of hygrothermal vibration analysis of functional graded nanoplates using nonlocal high-order continuum plate model (Yıldırım *et al.* 2024) and the thermomechanical buckling of FGM porous structures (Ertenli *et al.* 2024, Esen *et al.* 2024, Pehlivan *et al.* 2024).

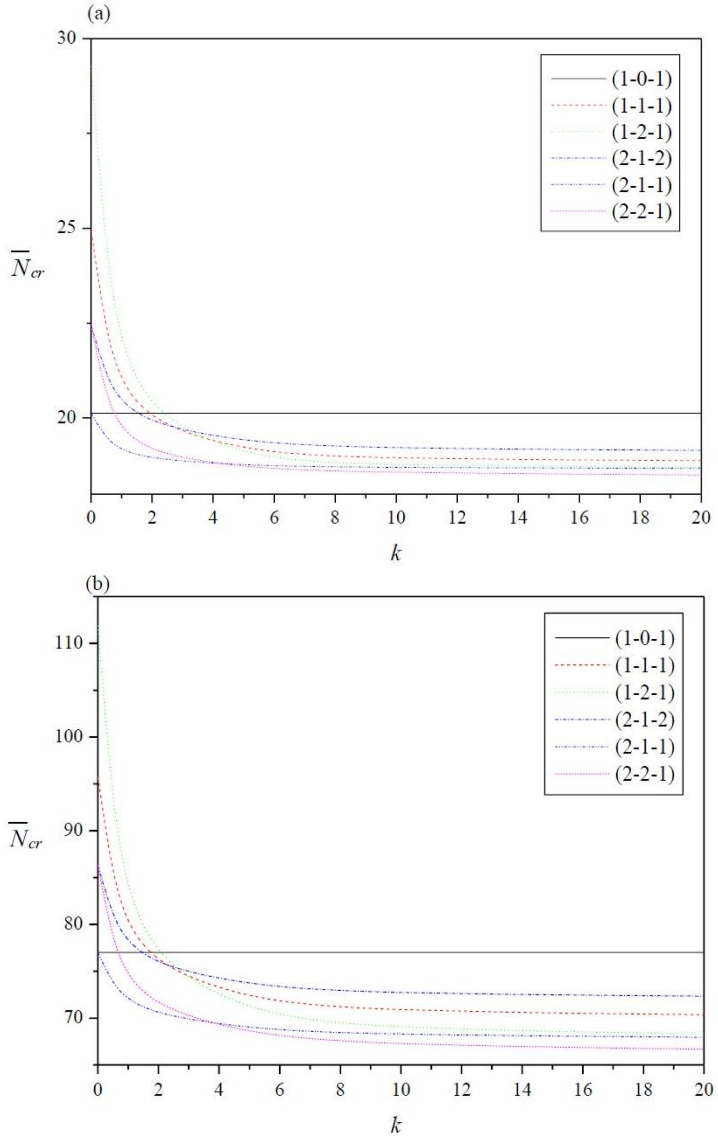

Fig. 5 Effect of the volume fraction index (k) on the nondimensional critical buckling load $\overline{N}_{cr}$ of FG sandwich beams type C: (a) simply supported beam and (b) clamped–clamped beam ($L/h = 10$)

References

Belabed, Z., Houari, M.S.A., Tounsi, A., Mahmoud, S.R. and Bég, O.A. (2014), "An efficient and simple higher order shear and normal deformation theory for functionally graded material (FGM) plates", *Compos. Part B: Eng.*, **60**, 274-283. https://doi.org/10.1016/j.compositesb.2013.12.057.

Belarbi, M.O., Benounas, S., Salami, S.J., Khechai, A., Daikh, A.A., Houari, M.S.A. and Bezzina, S. (2025), "An enhanced finite element model for static bending analysis of functionally graded plates with power-law, exponential, and sigmoid material gradients", *Arch. Appl. Mech.*, **95**(1), 1-24. https://doi.org/10.1007/s00419-024-02727-x.

Belouettar, S., Abbadi, A., Azari, Z., Belouettar, R. and Freres, P. (2009), "Experimental investigation of static and fatigue behaviour of composites honeycomb materials using four point bending tests", *Compos. Struct*., **87**(3), 265-273. https://doi.org/10.1016/j.compstruct.2008.01.015.

Birman, V. and Byrd, L.W. (2007), "Modeling and analysis of functionally graded materials and structures", *Appl. Mech. Rev*., **60**(5), 195-216. https://doi.org/10.1115/1.2777164.

Bouremana, M., Tounsi, A. and Adda-Bedia, E. (2013), "A new simple shear and normal deformations theory for functionally graded beams", *Steel Compos. Struct.*, **15**(5), 467-479. https://doi.org/10.12989/scs.2013.15.5.467.

Carrera, E., Miglioretti, F. and Petrolo, M. (2011), "Accuracy of refined finite elements for laminated plate analysis", *Compos. Struct*., **93**(5), 1311-1327. https://doi.org/10.1016/j.compstruct.2010.11.007.

Daikh, A.A., Drai, A., Bensaid, I., Houari, M.S.A. and Tounsi, A. (2021a), "On vibration of functionally graded sandwich nanoplates in the thermal environment", *J. Sandwich. Struct. Mater*., **23**(6), 2217-2244. https://doi.org/10.1177/1099636220909790

Daikh, A.A., Houari, M.S.A. and Eltaher, M.A. (2021b), "A novel nonlocal strain gradient quasi-3D bending analysis of sigmoid functionally graded sandwich nanoplates", *Compos. Struct.*, **262**, 113347. https://doi.org/10.1016/j.compstruct.2020.113347.

Ertenli, M.F. and Esen, İ. (2024), "The effect of the various porous layers on thermomechanical buckling of FGM sandwich plates", *Mech. Adv. Mater. Struct.*, **31**(28), 10935-10961. https://doi.org/10.1080/15376494.2023.2299934.

Esen, I., Garip, Z.S. and Eren, E. (2024), "The effects of the foam and FGM distributions on thermomechanical buckling response of sandwich plates", *Acta Mechanica*, **235**(2), 1319-1343. https://doi.org/10.1007/s00707-023-03808-8.

Foroutan, K. and Dai, L. (2022), "Post-buckling analysis of sandwich FG porous cylindrical shells with a viscoelastic core", *Steel Compos. Struct.*, **45**(3), 349-367. https://doi.org/10.12989/scs.2022.45.3.349.

Fortas, L., Messai, A., Merzouki, T. and Houari, M.S.A. (2022), "Elastic stability of functionally graded graphene reinforced porous nanocomposite beams using two variables shear deformation", *Steel Compos. Struct.*, **45**(3), 305-318. https://doi.org/10.12989/scs.2022.45.3.305.

Garg, A., Maji, A. and Talha, M. (2020), "Recent developments in modeling and analysis of functionally graded sandwich structures: A review", *Mech. Adv. Mater. Struct*., **27**(8), 684-703. https://doi.org/10.1080/15376494.2018.1517784.

Ghazi, Z.A. and Mehar, K. (2022), "Nonlinear flexural and vibration analysis of bidirectional functionally graded graphene oxide reinforced sandwich shell", *Steel Compos. Struct.*, **42**(3), 399-414. https://doi.org/10.12989/scs.2022.42.3.399.

Hirane, H., Belarbi, M.O., Houari, M.S.A. and Tounsi, A. (2021), "On the layerwise finite element formulation for static and free vibration analysis of functionally graded sandwich plates", *Eng. Comput*., 1-29. https://doi.org/10.1007/s00366-020-01250-1.

Jha, D.K., Kant, T. and Singh, R.K. (2013), "A critical review of recent research on functionally graded plates", *Compos. Struct.*, **96**, 833-849. https://doi.org/10.1016/j.compstruct.2012.09.001.

Karakoti, A., Pandey, S. and Kar, V.R. (2021), "Dynamic responses analysis of P and S-FGM sandwich cylindrical shell panels using a new layerwise method", *Struct. Eng. Mech*., **80**(4), 417-432. https://doi.org/10.12989/sem.2021.80.4.417.

Karamanlı, A. (2017), "Bending behaviour of two directional functionally graded sandwich beams by using a quasi-3d shear deformation theory", *Compos. Struct.*, **174**, 70-86. https://doi.org/10.1016/j.compstruct.2017.04.046.

Kolahchi, R. (2017), "A comparative study on the bending, vibration and buckling of viscoelastic sandwich nano-plates based on different nonlocal theories using DC, HDQ and DQ methods", *Aerosp. Sci. Technol*., **66**, 235-248. https://doi.org/10.1016/j.ast.2017.03.016.

Lal, D.K., Ghazi, Z.A., Mehar, K. and Panda, S.K. (2023), "Nonlinear thermal stability analysis of P-FGM sandwich doubly curved shell structure under variable temperature field", *Struct. Eng. Mech*., **87**(1), 65-80. https://doi.org/10.12989/sem.2023.87.1.065.

Le, K.C. and Tran, T.M. (2025), "Asymptotically exact theory of functionally graded elastic beams", *Int. J.*

Eng. Sci., **209**, 104214. https://doi.org/10.1016/j.ijengsci.2025.104214.
Li, Q., Iu, V.P. and Kou, K.P. (2008), "Three-dimensional vibration analysis of functionally graded material sandwich plates", *J. Sound. Vib.*, **311**(1), 498-515. https://doi.org/10.1016/j.jsv.2007.09.018.
Liang, D., Wu, Q., Lu, X. and Tahouneh, V. (2020), "Vibration behavior of trapezoidal sandwich plate with functionally graded-porous core and graphene platelet-reinforced layers", *Steel Compos. Struct.*, **36**(1), 47-62. https://doi.org/10.12989/scs.2020.36.1.047.
Merzouki, T., Houari, M.S.A., Bessaim, A., Haboussi, M., Dimitri, R. and Tornabene, F. (2022), "Bending analysis of functionally graded porous nanocomposite beams based on a non-local strain gradient theory", *Math. Mech. Solid.*, **27**(1), 66-92. https://doi.org/10.1177/10812865211011759.
Mittal, R.K., Kumar, A. and Singh, A.K. (2022), "Vibration analysis of FGM sandwich cylindrical shell using two variables refined higher-order theory", *Struct. Eng. Mech.*, **83**(5), 539-552. https://doi.org/10.12989/sem.2022.83.5.539.
Mokhefi, D., Bessaim, A., Houari, M.S.A., Deffane, Z., Houari-Belkadi, H., Ali, B., ... & Merzouki, T. (2024), "A nonlocal strain gradient model for buckling analysis of advanced FG CNT-reinforced composite nanobeams", *Couple. Syst. Mech.*, **13**(5), 375-393. https://doi.org/10.12989/csm.2024.13.5.375.
Mouffoki, A., Bedia, E.A., Houari, M.S.A., Tounsi, A. and Mahmoud, S.R. (2017), "Vibration analysis of nonlocal advanced nanobeams in hygro-thermal environment using a new two-unknown trigonometric shear deformation beam theory", *Smart Struct. Syst.*, **20**(3), 369-383. https://doi.org/10.12989/sss.2017.20.3.369.
Nguyen, T.H. and Nguyen, T.P. (2015), "A new approach to the analysis of free vibration, buckling and static of functionally graded sandwich beams using a higher-order shear deformation theory", *Int. J. Mech. Sci.*, **101-102**, 467-476. https://doi.org/10.1016/j.ijmecsci.2015.09.001.
Nguyen, T.K. and Nguyen, B.D. (2015), "A new higher-order shear deformation theory for static, buckling and free vibration analysis of functionally graded sandwich beams", *J. Sandwich. Struct. Mater.*, **17**(6), 613-631. https://doi.org/10.1177/1099636215589237.
Nguyen, T.K., Vo, T.P. and Thai, H.T. (2013), "Static and free vibration of axially loaded functionally graded beams based on the first-order shear deformation theory", *Compos. Part B. Eng.*, **55**, 147-157. https://doi.org/10.1016/j.compositesb.2013.06.011.
Osofero, A.I., Pasternak, H. and Klasztorny, M. (2009), "Advanced analysis of composite sandwich beams: a unified higher order beam theory", Easd Eurosteel, Graz, Austria.
Osofero, A.I., Pasternak, H. and Klasztorny, M. (2010), "A unified higher order beam theory for composite sandwich beams", *J. Sandw. Struct. Mater.*, **12**(1), 45-65. https://doi.org/10.1177/1099636209346613.
Pagani, A. and Sanchez-Majano, A.R. (2022), "Influence of fiber misalignments on buckling performance of variable stiffness composites using layerwise models and random fields", *Mech. Adv. Mater. Struct.*, **29**(3), 384-399. https://doi.org/10.1080/15376494.2020.1771485.
Pehlivan, F., Esen, I. and Aktas, K.G. (2024), "Thermomechanical response of smart magneto-electro-elastic FGM nanosensor beams with intended porosity", *Arab. J. Sci. Eng.*, 1-23. https://doi.org/10.1007/s13369-024-09197-x.
Sabherwal, P., Belarbi, M.O., Raman, R., Garg, A., Li, L., Devidas Chalak, H., ... & Avcar, M. (2024), "Free vibration analysis of laminated sandwich plates using wavelet finite element method", *AIAA J.*, **62**(2), 824-832. https://doi.org/10.2514/1.J063364.
Sahoo, B., Mehar, K., Sahoo, B., Sharma, N. and Panda, S.K. (2021), "Thermal frequency analysis of FG sandwich structure under variable temperature loading", *Struct. Eng. Mech.*, **77**(1), 57-74. https://doi.org/10.12989/sem.2021.77.1.057.
Sahu, S.K., Sreekanth, P.R. and Reddy, S.K. (2022), "A brief review on advanced sandwich structures with customized design core and composite face sheet", *Polym.*, **14**(20), 4267. https://doi.org/10.3390/polym14204267.
Sayyad, A.S. and Ghugal, Y.M. (2018), "Bending, buckling and free vibration of laminated composite and sandwich beams: A critical review of literature", *Compos. Struct.*, **171**, 486-504. https://doi.org/10.1016/j.compstruct.2017.10.013.
Shahmohammadi, M.A., Azhari, M. and Saadatpour, M.M. (2020), "Free vibration analysis of sandwich

FGM shells using isogeometric B-spline finite strip method", *Steel Compos. Struct.*, **34**(3), 361-376. https://doi.org/10.12989/scs.2020.34.3.361.

Shahmohammadi, M.A., Azhari, M., Saadatpour, M.M. and Sarrami-Foroushani, S. (2020), "Geometrically nonlinear analysis of sandwich FGM and laminated composite degenerated shells using the isogeometric finite strip method", *Comput. Meth. Appl. Mech. Eng.*, **371**, 113311. https://doi.org/10.1016/j.cma.2020.113311.

Shen, H.S. (2009), *Functionally Graded Materials: Nonlinear Analysis of Plates and Shells*, CRC Press, Boca Raton.

Si, H., Shen, D., Xia, J. and Tahouneh, V. (2020), "Vibration behavior of functionally graded sandwich beam with porous core and nanocomposite layers", *Steel Compos. Struct.*, **36**(1), 1-16. https://doi.org/10.12989/scs.2020.36.1.001.

Taskin, M.A. and Demirhan, N. (2021), "Three-dimensional analysis of functionally graded sandwich plates with simply supported boundary conditions", *Compos. Struct.*, **268**, 113932. https://doi.org/10.1016/j.compstruct.2021.113932.

Tounsi, A., Abdelhak, Z. and Adda Bedia, E. (2013), "An efficient higher-order shear and normal deformation theory for buckling analysis of functionally graded sandwich plates", *Steel Compos. Struct.*, **15**(1), 49-71. https://doi.org/10.12989/scs.2013.15.1.049.

Vel, S.S., Caccese, V. and Zhao, H. (2005), "Elastic coupling effects in tapered sandwich panels with laminated anisotropic composite facings", *J. Compos. Mater.*, **39**(24), 2161-2183. https://doi.org/10.1177/0021998305052033.

Vo, T.P., Thai, H.T., Nguyen, T.K., Maheri, A. and Lee, J. (2014), "Finite element model for vibration and buckling of functionally graded sandwich beams based on a refined shear deformation theory", *Eng. Struct.*, **64**, 12-22. https://doi.org/10.1016/j.engstruct.2014.01.029.

Wang, Z.X. and Shen, H.S. (2012), "Nonlinear vibration and bending of sandwich plates with nanotube-reinforced composite face sheets", *Compos. Part B Eng.*, **43**(2), 411-421. https://doi.org/10.1016/j.compositesb.2011.04.040.

Yıldırım, E. and Esen, I. (2024), "Effect of the porous structure on the hygrothermal vibration analysis of functional graded nanoplates using nonlocal high-order continuum plate model", *Acta Mechanica*, **235**(8), 5079-5106. https://doi.org/10.1007/s00707-024-03990-3.

Zenkour, A.M. (2019), "Bending analysis of a supported functionally graded viscoelastic sandwich beam with an elastic core resting on Pasternak's elastic foundations", *Aerosp. Sci. Technol.*, **84**, 1020-1032. https://doi.org/10.1016/j.ast.2018.11.034.

CC